

A triple-resonant coil system for inherently co-registered proton-, sodium- and chloride-MRI at 9.4T

F. Wetterling¹, S. Ansar², L. Tritschler², R. Kalayciyan¹, S. Kirsch¹, M. Fatar², S. Meairs², and L. R. Schad¹

¹Computer Assisted Clinical Medicine, Heidelberg University, Mannheim, Germany, ²Department of Neurology, Heidelberg University, Mannheim, Germany

INTRODUCTION: Combined and spatially-resolved ^{35}Cl and ^{23}Na MR signal measurements could provide additional information about the progression of stroke [1]. However, X-nuclei ^{35}Cl and ^{23}Na MRI suffers from low signal/noise (S/N) owed to their low *in vivo* concentration, fast transversal relaxation times, and low gyromagnetic ratio. In order to maximize the S/N in the X-nuclei channels a triple resonant coil design requires intelligent geometric and/or electronic decoupling of the resonance structures. Two geometrically decoupled $^{23}\text{Na}/^{39}\text{K}$ volume coils have been previously combined with an electronically-decoupled ^1H surface coil [2]. In a more recent study double-tuned $^1\text{H}/^{23}\text{Na}$ volume resonator was used in conjunction with a ^{35}Cl surface coil [1]. Since, the S/N benefits of surface coils over volume resonators are well-known [3] a double-tuned $^{23}\text{Na}/^{35}\text{Cl}$ surface coil was developed in this study in order to maximize both the ^{23}Na and the ^{35}Cl -channel's sensitivity, while ^1H MR capability was maintained through the use of a linear ^1H volume resonator. The advantages of combined ^{35}Cl , ^{23}Na , and ^1H MRI are demonstrated in this contribution by means of phantom and *in vivo* experiments.

METHODS: A two-winding double-tuned $^{23}\text{Na}/^{35}\text{Cl}$ (105.9 / 39.2 MHz) surface coil (i.d.: 20 and 30 mm) was developed (Figure 1) with $C_1=120\text{pF}$, $C_2=100\text{pF}$, $C_3=0.8\cdot6\text{pF}$, variable $L_1\sim35\mu\text{H}$, and $C_m=2.21\text{pF}$. Balanced variable tuning and matching was achieved by choosing virtual ground connection to be at half distance of the concentric-two-winding surface coil. Thus, capacitor splitting was rendered unnecessary and the number of capacitive elements could be held low – maintaining a high Q-factor. The loaded/unloaded Q-factor ratio was measured to be 122/112 (^{35}Cl) and 63/54 (^{23}Na), respectively. In order to geometrically decouple the developed surface coil from the ^1H birdcage resonator (Bruker BioSpin GmbH, Ettlingen), the B_1 -field vector of the birdcage was orthogonally arranged to the surface coil's normal vector. No change in Q-factor was observed when both resonance structures were combined to form the triple-resonant coil system. A 10mm diameter, 20mm length reference vial filled with 0.6% NaCl solution was permanently fixed on top of the surface coil for later inter-individual image co-registration purposes. ^1H T_2 mapping was performed using a multi slice multi echo (MSME) sequence with $TR = 15000\text{ ms}$, $TE = 20\text{ ms}$ to 400 ms in 20.2 ms increments, $0.78 \times 0.78\text{ mm}^2$ in-plane resolution with 3 axial slices of 2 mm thickness and an inter-slice distance of 4 mm. The total measurement time (TA) was 16 min. ^1H diffusion weighted imaging was performed using an echo planar imaging (EPI) sequence with $TR = 5000\text{ ms}$, $TE = 20\text{ ms}$, and b -values = 100 and 1000 s/mm^2 . The in-plane resolution was $0.2 \times 0.2\text{ mm}^2$ with 20 axial slices of 1.9 mm thickness, an inter-slice distance of 2 mm, and $TA = 2\text{ min 20 sec}$. A 3D Fast Low Angle Shot (FLASH) sequence on a Bruker BioSpec 94/20 system was used to achieve a TE of 2.1ms, with voxel resolutions of $0.5 \times 0.5 \times 2\text{ mm}^3$ for ^{23}Na -MRI, and $1 \times 1 \times 2\text{ mm}^3$ for ^{35}Cl -MRI (after two-fold 3D zero-filling), $TR = 20\text{ ms}$, $TA = 10\text{ min}$, $BW = 4\text{ kHz}$, and 10% partial echo acquisition. For phantom scans two vials (10mm i.d., 20mm length) one filled with 0.6% KCl solution and the other filled with demineralised water were used. In conjunction with the permanently fixed reference vial on top of the surface coil $^1\text{H}/^{23}\text{Na}/^{35}\text{Cl}$ phantom was formed. The *in vivo* experiments were carried out under appropriate animal license and ethics approval. Stroke was induced by right middle cerebral artery occlusion (MCAO) in one male Wistar rat (410g) using the intraluminal thread model. *In vivo* scanning was performed 5 days after MCAO.

RESULTS and DISCUSSION: Phantom experiments confirmed the superior functioning of the newly-developed triple resonant coil system without the appearance of imaging artifacts in either the ^{35}Cl , ^{23}Na , nor the ^1H MR images (Figure 2). Although S/N can be further improved by employing single-tuned ^{35}Cl and ^{23}Na surface coils, interchanging coils during a longitudinal $^{35}\text{Cl}/^{23}\text{Na}$ study increases the error rate (including errors in sample and coil re-positioning). Therefore restricted ^1H -sensitivity achieved with ^1H volume resonator was an acceptable trade-off for triple resonance MRI capability in order to maximize the X-nuclei sensitivity. The surface coil's performance could be further improved by lowering the coil's ambient temperature at the 9.4T field strength [4]. MR imaging of a rat stroke model at 5 days after MCAO demonstrated the strength of developed coil system. For the first time ^1H T_2 and apparent diffusion coefficient (ADC) maps as well as ^{23}Na and ^{35}Cl images were recorded (Figure 3) without the need to exchange coil systems during the time course of the experiment. The stroke region was defined as tissue with hyperintense ^{23}Na signal [5]. A similar anatomical region of interest (ROI) was chosen from contralateral normal hemisphere. A third ROI was selected to be within the reference vial. Mean and standard deviations were computed by averaging over the range of values collected for each ROI which can be found in Table 1. Hyperintense T_2 -weighted signal intensity was measured within the stroke lesion, whereas hyper- as well as hypointense ADC was measured within the stroke tissue, which resulted in a non-significant ADC compared to contralateral healthy tissue. The ambiguity of ^1H T_2 and ADC values during the chronic stroke phase have been reported previously [6]. Approximately 170% more ^{23}Na signal was measured in stroke compared to contralateral normal tissue. The ^{35}Cl signal was only elevated by $\sim 50\%$ in identical brain region. This difference was also reflected by measured non-unity (1.8) Na/Cl ratio in stroke tissue, while the Na/Cl ratio was measured to be nearly identical (~ 0.9) in the reference vial and contralateral tissue. Others reported differences in the Na/Cl ratio of blood (1.36) and muscle tissue (2.33) in frogs before [7]. Nevertheless, more experiments are required to confirm the physiological relevance of these findings, since herein reported difference in the Na/Cl ratio may result from either variation in actual ion concentration or from relaxation time variations for the ^{23}Na and ^{35}Cl -nuclei which were enclosed in either stroke or contralateral normal tissue. Future experiments must hence focus on employing short TE and long TR in order to firstly suppress relaxation time effects on measured Na/Cl ratio, secondly to clarify whether ^{23}Na and ^{35}Cl concentrations can change by different quantities after stroke and thirdly how it reflects pathophysiological processes in the ischaemic brain.

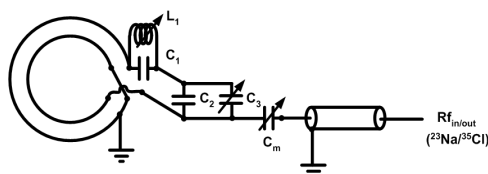


Figure 1: coil circuit.

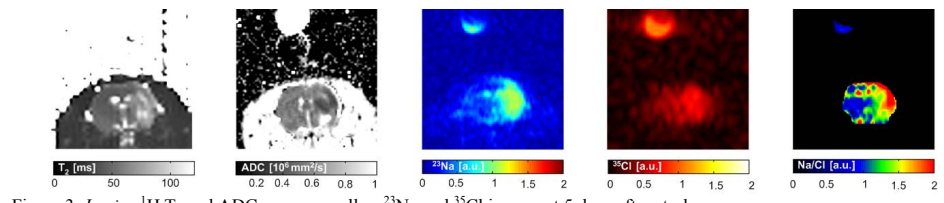


Figure 3: *In vivo* ^1H T_2 and ADC maps as well as ^{23}Na and ^{35}Cl images at 5 days after stroke.

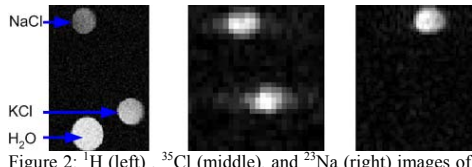


Figure 2: ^1H (left), ^{35}Cl (middle), and ^{23}Na (right) images of a phantom.

T_2 [ms]	ADC [$10^6\text{ m}^2/\text{s}$]	Na [a.u.]	Cl [a.u.]	Na/Cl [a.u.]	ROI
75 ± 14	0.6 ± 0.26	0.96 ± 0.01	0.6 ± 0.14	1.8 ± 0.55	stroke
45 ± 4	0.54 ± 0.37	0.35 ± 0.05	0.4 ± 0.06	0.85 ± 0.19	contralateral
303 ± 15	1.80 ± 0.30	0.94 ± 0.08	1.1 ± 0.005	0.89 ± 0.08	reference vial

Table 1: Mean and standard deviation for selected ROIs.

REFERENCES: [1] Kirsch *et al.*, NMR in Biomed 23, 592-600 (2010); [2] Augath *et al.*, JMR 200, 134-136 (2009); [3] Hayes *et al.*, Medical Physics 12, 604-607; [4] Baltes *et al.*, NMR in Biomed 22, 834-842 (2009); [5] Wetterling *et al.*, Proc. ISMRM 18, Stockholm, 680 (2010); [6] Miyasaka *et al.*, Radiology 215, 199-204 (2000); [7] Fennw *et al.*, Am. J. Physiol. 1701, p. 251